Comparison of the Physicochemical Characteristics of Bio-char Pyrolyzed from Moso Bamboo and Rice Husk with Different Pyrolysis Temperatures

Yimeng Zhang,[a] Zhongqing Ma,[b,*] Qisheng Zhang,[a] Jiayao Wang,[b] Qianqiang Ma,[b] Youyou Yang,[c] Xiping Luo,[c] and Weigang Zhang [b,*]

Bio-char pyrolyzed from biomass waste has been notably applied in various industries due to its versatile physicochemical characteristics. This paper investigated the difference of the properties of the bio-char derived from moso bamboo and rice husk under different pyrolysis temperatures (200 °C to 800 °C). As the temperature increased, the bio-char yield for both bamboo bio-char (BC) and rice husk bio-char (RHC) decreased, while the carbon element content and fixed carbon, the value of higher heating value (HHV) and pH increased for both BC and RHC. At 800 °C, BC had a higher HHV of 32.78 MJ/kg than RHC of 19.22 MJ/kg, while RHC had a higher yield of char (42.99 wt.%) than BC (26.3 wt.%) because of the higher ash content (47.51 wt.%) in RHC. SiO_2 was the dominant component in the ash of RHC, accounting for 86.26 wt.%. The surface area (S_{BET}) of RHC (331.23 m^2/g) was higher than BC (259.89 m^2/g). However, the graphitization degree of BC was higher than RHC at the same temperature. The systematic study on the evolution of the basic properties of BC and RHC will provide a good reference for their high value-added application.

Keywords: Moso bamboo; Rice husk; Bio-char; Pyrolysis; Characteristics

*Contact information: a: School of Materials Science and Engineering, Nanjing Forestry University, Nanjing, Jiangsu 210037, P. R. China; b: School of Engineering, Key Laboratory of Wood Science & Technology of Zhejiang Province, National Engineering & Technology Research Center of Wood-Based Resources Comprehensive Utilization, Zhejiang Agriculture & Forestry University, Lin'an, Zhejiang 311300, P. R. China; c: Zhejiang Agriculture & Forestry University, Lin'an, Zhejiang 311300, P. R. China; *Corresponding authors: mazqzafu@163.com; zhangwgzafu@163.com*

INTRODUCTION

Biomass is a promising, eco-friendly, and renewable source for generating energy, fuels, and chemicals that could partially replace fossil fuels to reduce the pressure of environmental pollution problems (Ma *et al.* 2012, 2015a). China is rich in biomass resources, mainly from agriculture and forestry residues. Bamboo and rice husk (RH) are the two typical biomass species in China with the largest annual production of 7 million and 40 million tonnes in the world, respectively (Paethanom and Yoshikawa 2012; Chen *et al.* 2014a). Compared to woody biomass, bamboo and rice husk have the advantage of a short growth period for harvesting, with growth periods of 3 to 5 years and 6 months, respectively. However, during the process of bamboo scrimber manufacturing and rice milling, a large proportion of these types of waste are produced, occupying approximately 30% and 20% of the initial weight, respectively (Alvarez *et al.* 2014; Chen *et al.* 2015a). Currently, this waste is simply used as fuel for burning in the boiler or as

fodder in the livestock breeding industry. Therefore, identifying how to increase value through additional utilization of this waste biomass is a strategic problem for the development of the bamboo manufacturing and rice milling industry.

Biomass pyrolysis is a thermochemical degradation process operating in an inert or very low stoichiometric oxygen atmosphere that converts solid biomass into three phase products, namely gaseous (combustible gas), liquid (bio-oil), and solid (bio-char) products (Yang *et al.* 2016; Chen *et al.* 2017a, 2017b). Compared to fast pyrolysis with a fast heating rate (generally over 300 °C/min) and short residence time (0.5 s to 10 s), the main product of slow pyrolysis with a moderate heating rate of 1 °C/min to 30 °C/min was the solid bio-char instead of the liquid bio-oil (Duman *et al.* 2011). Lower heating rates allow sufficient time for the molecule repolymerization reaction to occur from the three main components (cellulose, hemicellulose, and lignin), forming a polycyclic carbon structure and maximizing the yield of solid bio-char (Chen *et al.* 2012).

Bio-char as a recalcitrant carbonaceous material has been notably applied in some areas because of its versatile physicochemical characteristics. These promising potential applications include: energy production for a high heating value (Nanda *et al.* 2016), acid soil remediation because of its alkaline pH value and being rich in plant nutrients (Qian *et al.* 2015), carbon sequestration due to the high content of carbon (Rafiq *et al.* 2016), an excellent intermediate form for activated carbon production (Alvarez *et al.* 2014), or use as a catalyst precursor and fuel cell material for a strong pore structure and low electrical resistivity (Chen *et al.* 2015b). However, these applications are highly related to the basic properties of bio-char, which are significantly affected by the types of raw materials and the pyrolysis parameters (heating rate, solid residence time, and temperature, *etc.*) (Angin 2013a; Zhang *et al.* 2015). Thus, the study of the influence of the pyrolysis parameters on the basic properties of bio-char has attracted increasing attention.

Among various slow pyrolysis parameters (temperature, heating rate, and residence time), pyrolysis temperature is considered to be the most important parameter that significantly controls the yield and quality of the solid bio-char, including the chemical compositions, higher heating value (HHV), pH value, and pore structure (Kan *et al.* 2016; Tripathi *et al.* 2016). Using other biomass (not bamboo and RH), numerous tests have been performed on the effect of temperature on the properties of solid bio-char (Uçar and Karagöz 2009; Fu *et al.* 2011; Angin 2013a; Lee *et al.* 2013; Cimo *et al.* 2014; Luo *et al.* 2015; Zhang *et al.* 2015; Rafiq *et al.* 2016; Chen *et al.* 2016c). The basic evolution was that higher pyrolysis temperature would lead to lower bio-char yield and surface function groups content, higher HHV and pH value, and stronger pore structure. However, for the biomass of bamboo (Krzesińska and Zachariasz 2007; Kantarelis *et al.* 2010; Muhammad *et al.* 2012; Oyedun *et al.* 2013; Ren *et al.* 2013) and RH (Chen *et al.* 2014b; Yang *et al.* 2015; Zhang *et al.* 2016), most of the research was focused on the identification of pyrolysis behaviors and kinetics, and the components of volatiles (bio-oil and noncondensable gas) using thermogravimetric analysis-Fourier transform infrared spectrometry (TG-FTIR) and pyrolyzer-gas chromatography/mass spectrometer (Py-GC/MS). Furthermore, the amount of bio-char collected from this kind of analytical instrument was only at a milligram (mg) level, which was too small for further characterization of the other properties of bio-char. Therefore, a lab-scale tube furnace with a higher mass of bio-char at the gram (g) level was been employed in experiments for bio-char production. Using a tube furnace, Chen *et al.* (2014a) investigated the effect of bamboo pyrolysis temperature (300 °C to 700 °C) on the carbon and energy

distribution of the products. The variation of surface function groups and yield of RH bio-char at the temperature range of 600 °C to 900 °C was performed by Fu *et al.* (2011). Liu *et al.* (2011) also reported RH bio-char as presenting high adsorption capacity on the phenols. Alvarez *et al.* (2014) claimed that high quality activated carbon and amorphous silica could be produced using RH bio-char material. However, concerning the promising application of bio-char from bamboo and RH, some other important performance factors (chemical composition, functional group, pore structure, and crystallographic structure) under a wider range of pyrolysis temperatures still have been overlooked.

A systematic investigation was carried out to determine the effect of the pyrolysis temperature (200 °C, 300 °C, 400 °C, 500 °C, 600 °C, 700 °C, and 800 °C) on the yield and properties of bamboo bio-char (BC) and rice husk bio-char (RHC) was studied. Then, the comparison of the properties of BC and RHC was performed using Fourier transform infrared spectrometry (FTIR), thermogravimetric analysis (TGA), an X-ray diffractometer (XRD), gas sorption analyzer, *etc.*, to discuss their corresponding high value-added application in various industries.

EXPERIMENTAL

Materials

Five-year-old moso bamboo (*Phyllostachys edulis*) was harvested from the mountain in the Lin'an city of the Zhejiang Province in China. Then the outer and inner skin of bamboo was removed by a sander, and the middle part was kept for bio-char production. Another biomass, rice husk, was collected from a rice milling plant in the Jurong city of the Jiangsu Province.

The two types of biomass were first ground into powder, then screened using 160- and 200-mesh sieves. Finally, the powder with the particle size between 75 μm and 96 μm was kept and dried at 105 °C for 12 h for the pyrolysis experiment. The preparation process of bamboo and RH power is shown in Fig. 1.

Table 1. Contents of Cellulose, Hemicellulose, Lignin, and Extractives in the Dried Bamboo and Rice Husk

Samples	Holocellulose (wt.%)	Cellulose (wt.%)	Hemicellulose (wt.%)	Lignin (wt.%)	Extractives (wt.%)
Bamboo	70.51	47.29	23.21	20.13	5.11
Rice husk	59.88	40.19	19.69	14.43	4.32

After drying, the contents of cellulose, hemicellulose, lignin, and extractives in the bamboo and RH were tested. The content of extractives was determined using benzene-ethanol extraction according to the standard of GB/T 2677.6-94. The content of acid-insoluble lignin was determined by the standard of GB/T 2677.8-94. The content of cellulose was determined by nitric acid-alcohol method. The content of holocellulose was determined by the sodium chlorite method according to the standard of GB/T 2677.10-95. Then the content of hemicellulose was determined by Eq. 1.

$$\text{Hemicellulose (wt\%)} = \text{Holocellulose (wt\%)} - \text{Cellulose (wt\%)} \quad (1)$$

The results are shown in Table 1.

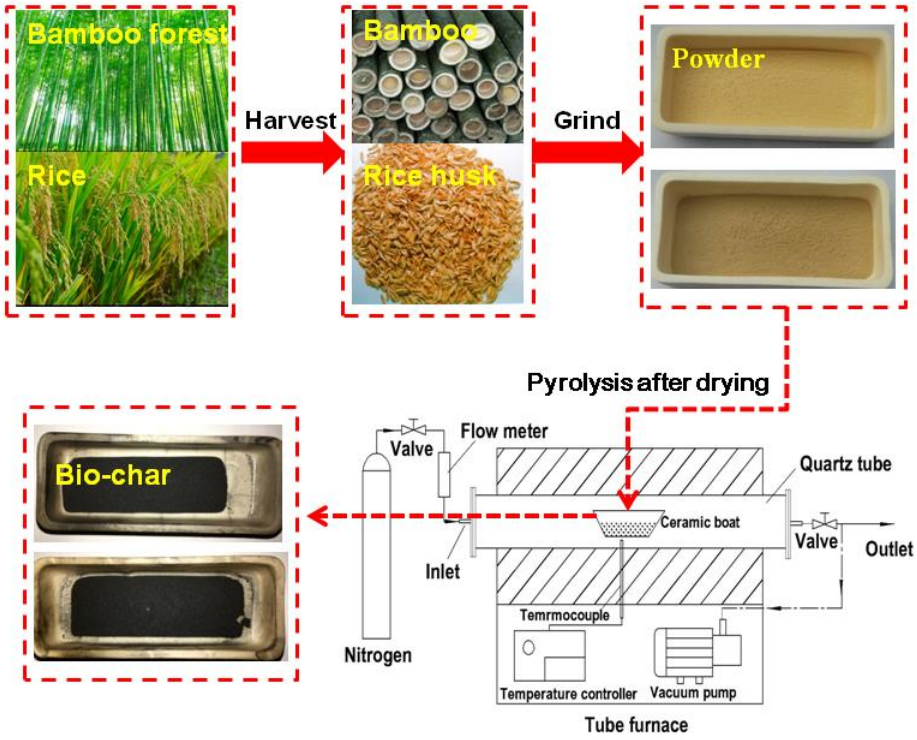

Fig. 1. Schematic diagram of biomass pyrolysis experiment

Pyrolysis experiment

An electrical heating tube furnace (Nanjing BYT Company, Nanjing, China, model number TL1200) was used to perform the biomass pyrolysis experiment, and its schematic diagram is shown in Fig. 1. As shown, the inner diameter and the length of the quartz tube were 60-mm and 1000-mm, respectively. In each experiment two ceramic boats (containing about 5 g of biomass powder in each boat) were put in the center of the quartz tube. Then the vacuum pump was used to extract all the air in the quartz tube. Next, the carrier (high-purity N_2) was injected into the quartz tube until it reached atmospheric pressure. Finally, the furnace was heated to the temperatures of 200 °C, 300 °C, 400 °C, 500 °C, 600 °C, 700 °C, and 800 °C at a fixed heating rate (10 °C/min) and a fixed flow rate (300 mL/min) of carrier gas. The terminal temperature was kept for 1 h. Once the temperature was cooled to room temperature using high-purity N_2, the bio-char was taken out for calculation of the yield and further analysis of its physicochemical characteristics. The average yield of bio-char was obtained from the data from at least three experiments.

Methods

Characteristics of bio-char

The ultimate analysis was conducted using an elemental analyzer (Vario EL III, Elementar, Langenselbold, Germany) following the CHNS/O model. Other mineral element content in the ash was tested with X-ray fluorescence (Axiosm AX-Petro, Rotterdam, Netherlands). The proximate analysis of bio-char was tested according to ASTM D1762-84 (2013). The heating value of bio-char was tested using an automatic calorimeter (ZDHW-300A, Hebi Keda Instrument & Meters Co., LTD, China). The pH

value was tested according to the Chinese national standard GB/T 12496.7 (1999). In each test, 2.5 g bio-char was mixed with 50 mL of deionized water to form the suspension. Then the suspension was heated to boiling, which was maintained for 5 min. Next, the suspension was filtered to remove the bio-char powder. Finally, the pH value of the filtrate was tested using a pH meter (pHS-25, Shanghai Leici Company, Shanghai, China) until it was cooled to the room temperature.

The surface chemical functional groups of the bio-char were tested using Fourier transform infrared spectrometry (Nicolet 6700, Thermo Fisher Scientific, Waltham, Massachusetts, USA). The thermal stability of the bio-char was analyzed using a thermogravimetric analyzer (TG209F1, Netzsch Instruments, Bavaria, Germany), and the terminal temperature was set as 1000 ℃ at a heating rate of 10 °C /min and a flow rate of high-purity nitrogen of 100 ml/min. The surface area and pore size distribution were obtained by using a Gas Sorption Analyzer (ASAP2020, Quantachrome Instruments Co., Ltd., Boynton Beach, Florida, USA). The specific surface area (S_{BET}), micro pore volume (V_{mic}), and mesopore volume (V_{mes}) were determined by way of the Brunauer-Emmett-Teller (BET) method, the t-plot method, and the Barrett-Joyner-Halenda (BJH) method, respectively. The crystallographic structure was tested using an X-ray diffractometer (XRD 6000, Shimadzu, Kyoto, Japan).

RESULTS AND DISCUSSION

Biochar Yields, Proximate and Ultimate Analysis, pH Value

Table 2 shows the effect of pyrolysis temperature on the yield, proximate analysis, HHV, and pH of BC and RHC. The yield decreased as the temperature increased for both BC and RHC because more solid substance was converted into lower molecular components, such as gaseous bio-gas and liquid bio-oil (Zhang *et al.* 2015). It is worth noting that compared to temperatures over 400 °C, larger weight loss (66.93 wt.% for BC and 47.65 wt.% for RHC) was observed before 400 °C. This result might be explained by the thermal degradation behaviors of three main components (cellulose, hemicellulose, and lignin). The contents of three main components in bamboo and RH are shown in Table 1.

According to the thermogravimetric analysis (TGA) of the three-component biomass, shown in Fig. 2, the main degradation temperatures were less than 400 °C along with 92 wt.%, 62 wt.%, and 35 wt.% weight loss for cellulose, hemicellulose, and lignin, respectively. However, the yield of RHC was much higher than BC at the same temperature. This was attributed to the higher ash content and lower volatile content in RHC, based on the result of the proximate analysis.

The HHV of BC and RHC increased from 19.47 MJ/kg and 15.54 MJ/kg to 32.78 MJ/kg and 19.22 MJ/kg, respectively, as the temperature was raised from 200 °C to 800 °C. This might be attributed to an increase of the fixed carbon content in the bio-char. However, the HHV of BC was much higher than RHC at the same temperature. More importantly, the HHV of the samples of BC-400, -500, -600, -700, and -800 were all higher than the standard coal (29.31 MJ/kg) (Majumder *et al*. 2008), which made the BC become a high-quality solid fuel that could be substituted for coal used in a boiler or used for barbecue char.

Table 2. Effect of Pyrolysis Temperature on the Proximate Analysis, HHV, and pH Value of BC and RHC

Samples	Yield (wt.%)	Volatiles (wt.%, db)	Fixed Carbon (wt.%, db)	Ash (wt.%, db)	HHV (MJ/kg)	pH
B-control	100	81.26 ± 0.19	17.14 ± 0.21	1.6 ± 0.08	19.29 ± 0.12	5.05 ± 0.15
BC-200	95.89 ± 1.46	82.72 ± 0.18	15.54 ± 0.27	1.74 ± 0.02	19.47 ± 0.14	5.46 ± 0.25
BC-300	46.67 ± 1.32	70.17 ± 1.28	26.59 ± 1.25	3.24 ± 0.03	24.99 ± 0.16	7.12 ± 0.33
BC-400	33.07 ± 0.13	40.41 ± 0.46	55.71 ± 0.47	3.88 ± 0.01	29.96 ± 0.23	9.01 ± 0.14
BC-500	29.43 ± 0.33	15.75 ± 0.22	80.19 ± 0.15	4.06 ± 0.06	31.73 ± 0.35	9.34 ± 0.36
BC-600	27.84 ± 0.31	10.24 ± 0.31	85.48 ± 0.38	4.28 ± 0.07	32.15 ± 0.24	9.88 ± 0.34
BC-700	27.1 ± 0.71	7.32 ± 0.40	88.28 ± 0.43	4.40 ± 0.03	32.55 ± 0.37	9.91 ± 0.27
BC-800	26.3 ± 0.43	6.36 ± 0.14	89.08 ± 0.4	4.56 ± 0.26	32.78 ± 0.78	10.18 ± 0.26
RH-control	100	64.71 ± 0.14	16.11 ± 0.15	19.18 ± 0.05	15.10 ± 0.28	4.91 ± 0.19
RHC-200	98.22 ± 0.31	57.2 ± 0.23	15.23 ± 0.17	27.57 ± 0.01	15.54 ± 0.14	6.14 ± 0.26
RHC-300	66.76 ± 1.24	38.92 ± 0.03	27.75 ± 0.21	33.33 ± 0.03	17.19 ± 0.19	6.83 ± 0.15
RHC-400	52.35 ± 0.44	17.98 ± 0.26	43.35 ± 0.19	38.67 ± 0.01	18.04 ± 0.23	7.75 ± 0.14
RHC-500	47.49 ± 0.61	9.81 ± 0.05	47.09 ± 0.31	43.1 ± 0.04	18.17 ± 0.22	8.60 ± 0.25
RHC-600	44.96 ± 0.66	6.13 ± 0.12	48.93 ± 0.34	44.94 ± 0.08	18.88 ± 0.16	9.22 ± 0.34
RHC-700	44.36 ± 0.84	4.69 ± 0.03	49.11 ± 0.56	46.20 ± 0.06	19.12 ± 0.36	10.00 ± 0.27
RHC-800	42.99 ± 0.39	3.29 ± 0.03	49.20 ± 0.66	47.51 ± 0.04	19.22 ± 0.34	10.08 ± 0.33

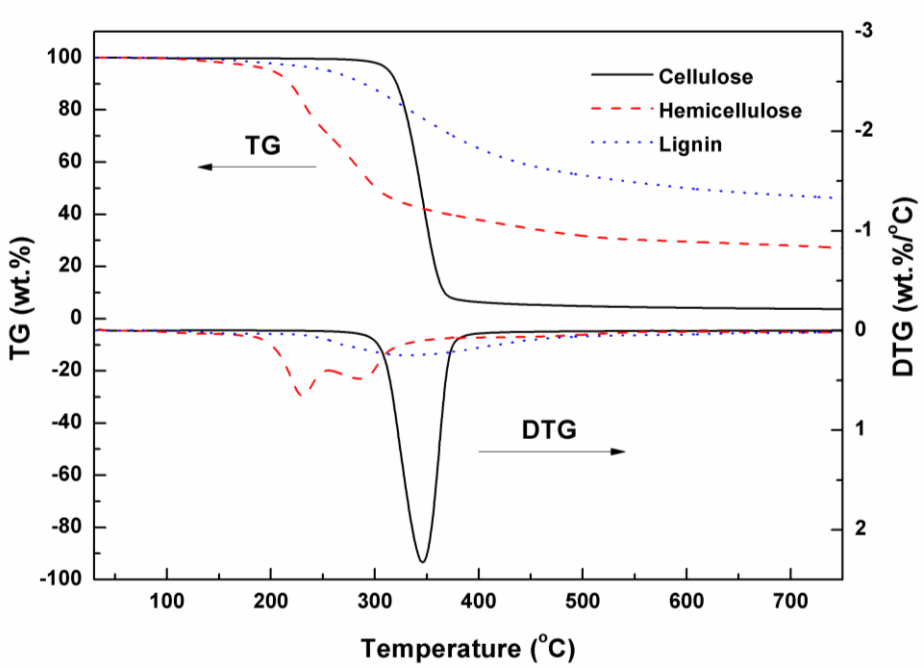

Fig. 2. Thermogravimetric analysis of cellulose, hemicellulose, and lignin at the heating rate of 10 °C/min

Table 3 shows the content of elements in the ash for BC-800 and RHC-800. Comparison of the pH value of bio-chars can be investigated after determination of the content of the alkali and alkali earth metals in the ash. The pH value of BC and RHC rose from 5.46 and 6.14 to 10.18 and 10.08, respectively, as the temperature was raised from 200 °C to 800 °C. This might be attributed to the increasing content of ash, which is rich in alkali and alkali earth metals (*e.g.* K, Ca, Na, and Mg), as shown in Table 2. Therefore, due to the strong alkalinity of BC and RHC, it could be used as a soil amendment to neutralize acidic soil in agriculture.

As shown in Table 3, the content of SiO_2 in the RHC-800 reached 86.26 wt.% which was much higher than BC-800. Based on the SEM images of RHC, Ma *et al.* (2015b) reported that the SiO_2 mainly presented on the outside and internal surface of the RHC at an amorphous structure. Alvarez *et al.* (2014) claimed that RHC from pyrolysis was a potential material from which to extract high purity amorphous silica that could be used in the zeolite catalyst, silica gel, or glass.

Table 3. Mass Percentage of Elements in the Ash of BC-800 and RHC-800

Samples	Element Contents in the Biomass Ash (wt.%)										
	CaO	Fe_2O_3	K_2O	MgO	Na_2O	SO_3	Cl	P_2O_5	SiO_2	Al_2O_3	Total
BC-800	0.96	0.39	21.09	2.29	0.10	6.88	2.69	4.56	5.25	n.d.[a]	44.21
RHC-800	1.09	0.69	3.08	0.46	0.07	1.15	1.25	0.38	86.26	0.17	94.60

n.d.[a]: not detected

Table 4. Effect of Pyrolysis Temperature on the Ultimate Analysis of BC and RHC

Samples	Carbon (wt.%)	Hydrogen (wt.%)	Nitrogen (wt.%)	Oxygen (wt.%)	H/C	O/C
B-control	47.66 ± 0.21	6.18 ± 0.01	0.15 ± 0.02	46.01 ± 0.22	0.13	0.97
BC-200	48.56 ± 0.28	6.11 ± 0.01	0.16 ± 0.01	45.17 ± 0.28	0.13	0.93
BC-300	63.06 ± 0.30	5.44 ± 0.03	0.17 ± 0.01	31.33 ± 0.24	0.09	0.50
BC-400	74.69 ± 0.23	4.17 ± 0.02	0.19 ± 0.03	20.95 ± 0.22	0.06	0.28
BC-500	84.20 ± 0.11	3.40 ± 0.01	0.25 ± 0.03	12.15 ± 0.16	0.04	0.14
BC-600	86.42 ± 0.13	2.61 ± 0.01	0.27 ± 0.05	10.70 ± 0.09	0.03	0.12
BC-700	88.15 ± 0.31	1.77 ± 0.03	0.44 ± 0.03	9.64 ± 0.81	0.02	0.11
BC-800	89.63 ± 0.35	1.44 ± 0.02	0.47 ± 0.03	8.46 ± 0.92	0.02	0.09
RH-control	38.19 ± 0.14	5.30 ± 0.02	0.28 ± 0.01	56.23 ± 0.15	0.14	1.47
RHC-200	34.91 ± 0.06	4.80 ± 0.01	0.34 ± 0.01	59.95 ± 0.06	0.14	1.72
RHC-300	39.78 ± 0.01	3.96 ± 0.01	0.35 ± 0.01	55.91 ± 0.01	0.10	1.41
RHC-400	40.44 ± 0.05	2.75 ± 0.10	0.46 ± 0.01	56.35 ± 0.04	0.07	1.39
RHC-500	40.90 ± 0.01	2.08 ± 0.10	0.49 ± 0.03	56.53 ± 0.02	0.05	1.38
RHC-600	42.17 ± 0.18	1.61 ± 0.10	0.50 ± 0.01	55.72 ± 0.18	0.04	1.32
RHC-700	42.82 ± 0.13	1.2 ± 0.02	0.52 ± 0.01	55.46 ± 0.13	0.03	1.30
RHC-800	43.95 ± 0.64	0.99 ± 0.05	0.55 ± 0.02	54.51 ± 0.57	0.02	1.24

The effect of the pyrolysis temperature on the elemental content (C, H, O, and N) is shown in Table 4. The carbon and nitrogen content of the bio-chars increased when the temperature increased, while the hydrogen and oxygen content decreased. Meanwhile the atomic ratio of H/C and O/C gradually decreased. This result indicated that more aromatic and carbonaceous components formed in the BC and RHC (Chen *et al.* 2012).

However, the content of carbon element in the BC was much higher than that of RHC at the same temperature. For the sample of BC-800, the content of carbon would reach nearly 90 wt.%, which was twice the content of carbon in the sample of RHC-800 (43.95 wt.%). The BC had lower ash content than RHC. This was also valid evidence to indicate that BC had a higher HHV than RHC. Also, the results indicated that BC had the stronger capacity for carbon sequestration.

FTIR Analysis

Figure 3 shows the effect of the pyrolysis temperature on the chemical functional groups of the BC and RHC. The infrared spectra showed 5 principal bands. The band at the wavenumbers of 3600 cm^{-1} to 3200 cm^{-1} was the most remarkable, being attributed to the stretching vibration of O-H (Ma *et al.* 2015a). The absorbance peak located between 3000 cm^{-1} and 2700 cm^{-1} was related to the stretching vibration of C-H, which mainly

came from aliphatic $–CH_2$ and alkanes $–CH_3$ (Ma *et al.* 2016). The stretch band at 1705 cm^{-1} was presented as the stretching vibration of C=O from the carboxyl and carbonyl groups (Chen *et al.* 2015a). The absorbance peak between 1690 cm^{-1} to 1450 cm^{-1} was the stretching vibration of C=C benzene ring skeleton mainly from aromatics (Chen *et al.* 2014b). The absorbance peak between 1200 cm^{-1} to 1000 cm^{-1} was caused by the stretching vibration of C-O from phenols (Chen *et al.* 2012).

As shown in Fig. 3, the intensity of absorbance from all functional groups in BC and RHC gradually decreased as the temperature was increased from 200 °C to 800 °C. At the lower pyrolysis temperatures (200 °C and 300 °C), these kinds of functional groups were still clearly observable in the BC and RHC. However, as the temperature was increased over 400 °C, some characteristic functional groups, such as hydroxyl, carboxyl, carbonyl, and methoxyl, gradually fell off under thermal cracking and were transformed into gaseous components (CO, CO_2, H_2, and CH_4,) and liquid components (acids, aldehydes, and phenols) (Ren *et al.* 2013). Finally, when the temperature reached 700 °C and 800 °C, the FTIR curves were almost flat. This finding was also supported by other researchers using pinewood (Luo *et al.* 2015), white ash (Chen *et al.* 2016d), and walnut (Zhao *et al.* 2016).

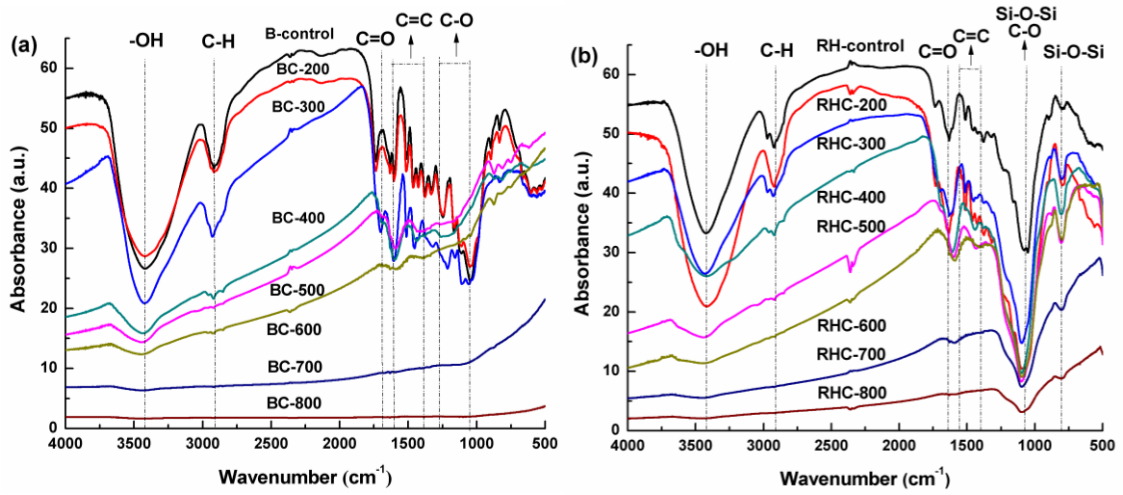

Fig. 3. The effect of pyrolysis temperature on the chemical functional groups

In Fig. 3 (b), due to the high content of SiO_2 in the RHC, the asymmetric stretching vibration of Si-O-Si was observed at the wavenumbers between 1200 cm^{-1} to 1050 cm^{-1}, and the characteristic absorbance peaks were at 1086 cm^{-1} and 1168 cm^{-1}. The symmetric stretching vibration of Si-O-Si was between 820 cm^{-1} and 760 cm^{-1}, and the characteristic absorbance peaks were at 795 cm^{-1} and 515 cm^{-1}. These bands for Si-O-Si stretching vibration in RHC were stronger than BC, indicating that the content of SiO_2 in the RHC was higher than BC.

TG Analysis

The thermal stability of the BC and RHC was tested using the thermogravimetric analyzer. Figure 4 shows the TG and DTG curves of BC (B-control, BC-200, -400, -600, and -800) and RHC (RH-control, RHC-200, -400, -600, and -800) at the heating rate of

20 °C/min with the 100 mL/min of high-purity nitrogen. The characteristic points of the TG and DTG curves are shown in Table 5. For both BC and RHC, the mass fraction of solid residues increased as the pyrolysis temperature increased, but RHC had a higher content of solid residues at the same temperature because of the higher ash content in RHC based on the proximate analysis in Table 2.

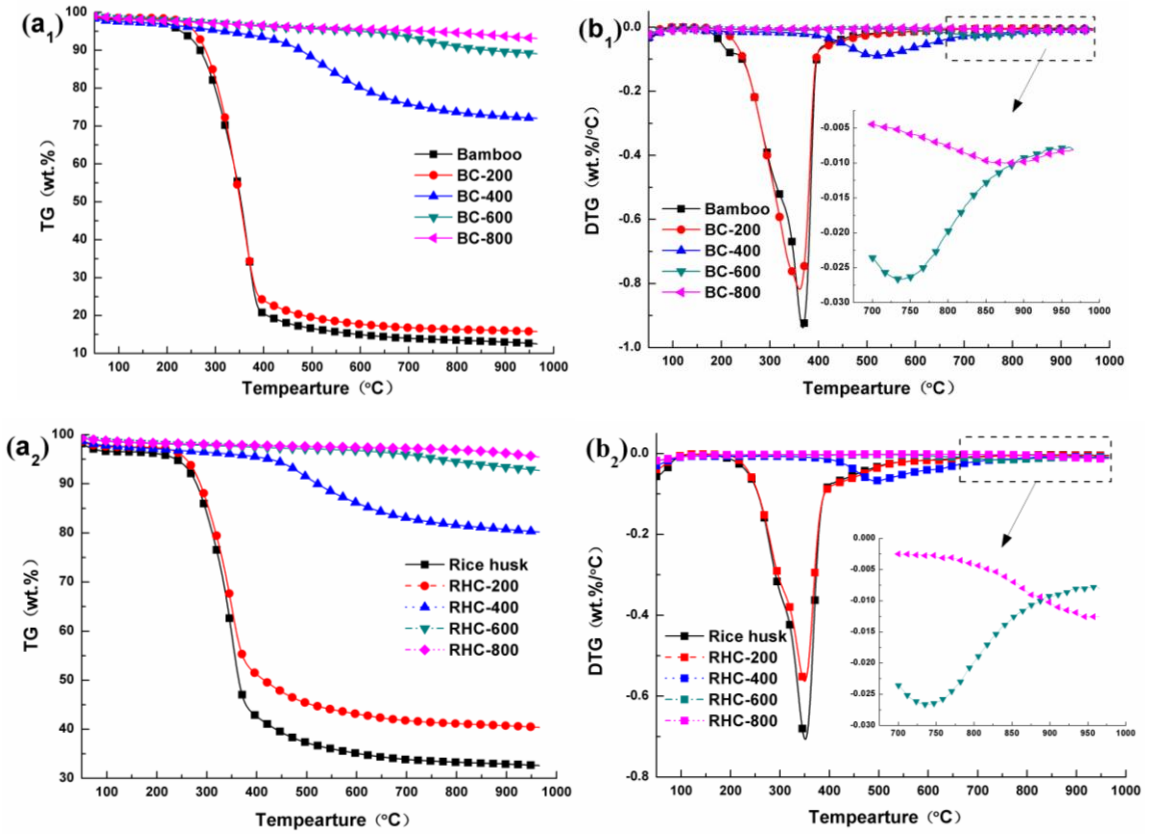

Fig. 4. Thermogravimetric analysis of BC (a_1 and b_1) and RHC (a_2 and b_2) from different pyrolysis temperatures: TG (a) and DTG (b) curves

The weight loss rate at the peak temperature decreased from 0.82 wt.%/°C to 0.011 wt.%/°C for BC and 0.57 wt.%/°C to 0.013 wt.%/°C for RHC. This result was caused by a decrease in the contents of degradable components in the bio-char, such as cellulose, hemicellulose, and lignin. During carbonization process of biomass, large amounts of functional groups fell off, and more components were polymerized into polyaromatic components with large molecular weight that were hard to degrade. However, BC had a higher weight loss rate than RHC because of the higher volatile content in BC. In addition, the peak temperature and the main weight loss region shifted toward the side of the higher temperature.

Overall, the thermal stability was considerably improved as the pyrolysis temperature increased, presenting a higher content of solid residues, a lower weight loss rate, and a higher peak temperature. This conclusion was also confirmed by Chen *et al.* (2016d).

Table 5. The Characteristic Point of TG/DTG Curves from BC and RHC

Samples	Residues Content (wt.%)	Main Weight Loss Range (°C)	Peak Temperature (°C)	Weight Loss Rate at Peak (wt.%/ °C)
B-control	12.53	155 to 461	359	0.93
BC-200	15.77	215 to 465	354	0.82
BC-400	72.03	362 to 743	531	0.08
BC-600	89.08	650 to 940	776	0.026
BC-800	93.12	700 to 960	881	0.011
RH-control	32.61	175 to 475	353	0.72
RHC-200	40.39	185 to 490	351	0.57
RHC-400	80.18	365 to 765	495	0.07
RHC-600	92.76	663 to 944	732	0.027
RHC-800	95.46	755 to 960	943	0.013

XRD Analysis

Figure 5 shows results of the XRD analysis of the BC and RHC from different pyrolysis temperatures. Three diffraction peaks are clearly shown in Fig. 5. At lower temperatures (control and 200 °C) for both BC and RHC, two sharp peaks at the 2θ of 16° and 22° were clearly observed, which represented the typical crystalline structure of the cellulose I_α (triclinic) and cellulose I_β (monoclinic), respectively (Wada *et al.* 2010). However, as the temperature continuously increased over 300 °C, the two sharp peaks gradually turned into one dispersion peak. This was caused by the thermal degradation of cellulose that was converted to amorphous carbon and aliphatic side chains.

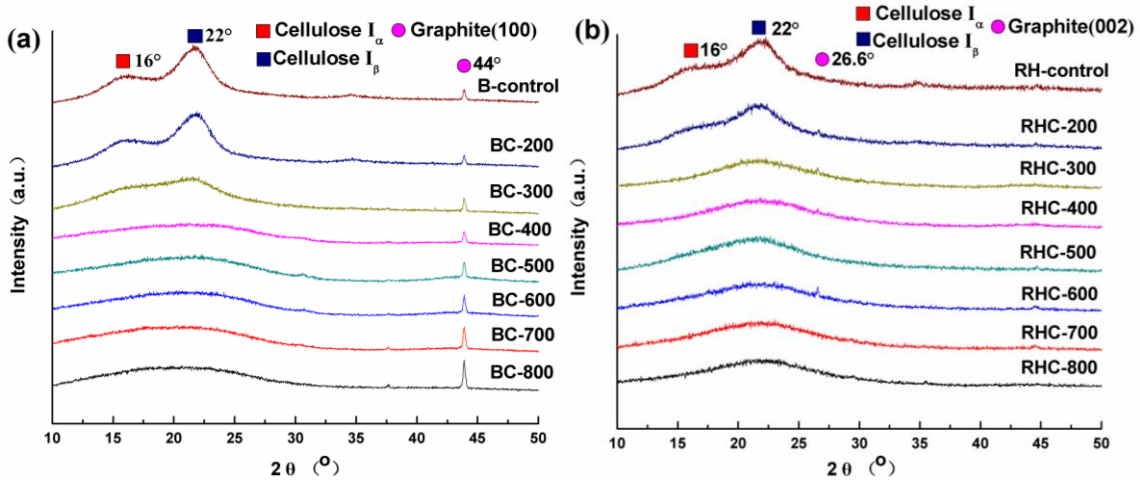

Fig. 5. XRD analysis of BC (a) and RHC (b) from different pyrolysis temperatures

The two other peaks observed at the 2θ values of 26.6° (from RHC) and 44° (from BC) were the graphite (002) and (100) bands, respectively (Fu *et al.* 2011). Guerrero *et*

al. (2008) reported that the (002) peak was attributable to the stacking of the graphitic basal planes of bio-char, while the (100) peak was related to the graphite-like atomic order within a single plane. As shown in Fig. 5 (b) for RHC, the intensity of the (002) peak was very weak. However the intensity of the (100) peak for BC was very strong, and it gradually increased as the pyrolysis temperature increased. This indicated that BC had a higher degree of graphitization than RHC. In addition, higher temperature leads to the formation of a graphite microcrystalline structure for BC (Yang *et al.* 2016). Then, the high graphitization degree resulted in high electrical conductivity in the bio-char. This also indicated that the BC was a more suitable electrode material for use in fuel cells than RHC.

Pore Structure Analysis

The specific surface area (S_{BET}), pore volume (V), and pore size distribution were the key parameters to evaluate the pore structure of biochar. Figure 6 shows the nitrogen adsorption-desorption isotherms of BC and RHC from different pyrolysis temperatures. According to the IUPAC classification, the types of adsorption isotherms can be divided into five classifications: type I(Henry), type II (Langmuir), type III (Freundlich), type IV (Brunauer-Emmett-Teller), and type V (stepped) . Then the type of adsorption isotherms of BC and RHC might be a mixture of types I and IV. Type I was attributed to the micropore structure, while the type IV was mainly caused by the mixture of micropore and mesopore structures. However, the adsorption-desorption isotherms of BC and RHC were not closed curves at the starting point of left side, which was significantly differentiated with the isotherms from activated carbon material (Angin *et al*. 2013b). This might be caused by the tar components remaining in the pore of bio-char and could not be completely desorbed by liquid nitrogen (Ma *et al*. 2015b).

The evolution of the pore structure of BC and RHC at various temperatures is shown in Table 6, and can be divided into three stages. For the first stage at the lower pyrolysis temperatures (200 °C to 500 °C), the value of S_{BET} for both BC and RHC had a slight increase compared to the control sample (bamboo and RH). In this stage, the maximum value of S_{BET} for BC and RHC was 57.09 and 39.05 m^2/g, respectively. The total pore volume consisted mainly of the mesopore (2 nm to 50 nm) volume, and the micropore (0 nm to 2 nm) could not be detected. In this temperature range, many volatiles were released from the thermal degradation of the cellulose and hemicellulose. However, the pore structure did not change remarkably. In the second stage at the middle pyrolysis temperature (600 °C), during the continuous degradation of lignin, substantial variation related to the pore structure occurred. Additionally, more "2D structure(s) of fused rings" formed (Yang *et al.* 2016). The S_{BET} for BC and RHC sharply increased to 127.41 m^2/g and 61.26 m^2/g, respectively. It was noteworthy that the micropore volume was detected, and the average pore size gradually decreased. This indicated that the micropore structure gradually replaced the mesopore structure as the temperature increased.

In the last stage, at high pyrolysis temperatures (700 °C to 800 °C), the "2D structure of fused rings" was transferred into the graphite microcrystalline structure. At this stage, the S_{BET} for BC and RHC reached their maximum values of 259.89 m^2/g and 331.23 m^2/g, respectively; the rate of micropore volume (V_{Mic}/V_{Tot}) also reached its maximum values. However, compared with other bio-char, the maximum S_{BET} of BC and

RHC was slightly lower than pine nut shell bio-char (433.1 m^2/g) (Chen *et al.* 2016a) and poplar wood bio-char (411.06 m^2/g) (Chen *et al.* 2016b).

Table 6. Pore Structure Analysis of BC and RHC from Different Pyrolysis Temperatures

Samples	Surface Area (S_{BET}, m^2/g)	Total Volume (V_{Tot},cm^3/g)	Micropore Volume (V_{Mic}, cm^3/g)	Mesopore Volume (V_{Mes},cm^3/g)	Micropore Rate (V_{Mic}/V_{Tot}, %)	Average Pore Size (nm)
B-control	4.52	0.011	0.003	0.007	27.27	9.62
BC-200	55.67	0.065	n.d. *	0.063	n.d.	25.82
BC-300	35.55	0.025	n.d.	0.023	n.d.	33.77
BC-400	52.35	0.045	n.d.	0.043	n.d.	26.97
BC-500	57.09	0.089	n.d.	0.085	n.d.	23.41
BC-600	127.41	0.141	0.005	0.092	3.55	22.42
BC-700	188.51	0.199	0.014	0.135	7.04	21.11
BC-800	259.89	0.236	0.047	0.139	19.92	18.14
RH-control	9.52	0.035	0.003	0.031	8.57	72.97
RHC-200	39.05	0.075	n.d.	0.074	n.d.	27.23
RHC-300	17.72	0.029	n.d.	0.028	n.d.	32.38
RHC-400	17.93	0.063	n.d.	0.061	n.d.	33.43
RHC-500	15.74	0.022	n.d.	0.021	n.d.	35.25
RHC-600	61.26	0.082	0.011	0.060	13.41	26.83
RHC-700	220.63	0.212	0.061	0.127	28.77	22.17
RHC-800	331.23	0.367	0.174	0.156	47.41	19.35

n.d.* : not detected

The differences in BET results might be caused by the different biomass materials and operating conditions (temperature, flow rate of carrier gas, residence time, *etc*.) of pyrolysis.

The increase of S_{BET} and micropore volume in the BC and RHC was mainly attributed to two pathways: (1) the release of the volatiles from the biomass' three components, especially from the degradation of benzene-ring linked compounds in the lignin; (2) The gap or crack from the formation process of the fused ring and the graphite microcrystals in the BC and RHC. Concerning the strong pore structure of BC and RHC, it could be a good adsorbent for use in sewage treatment.

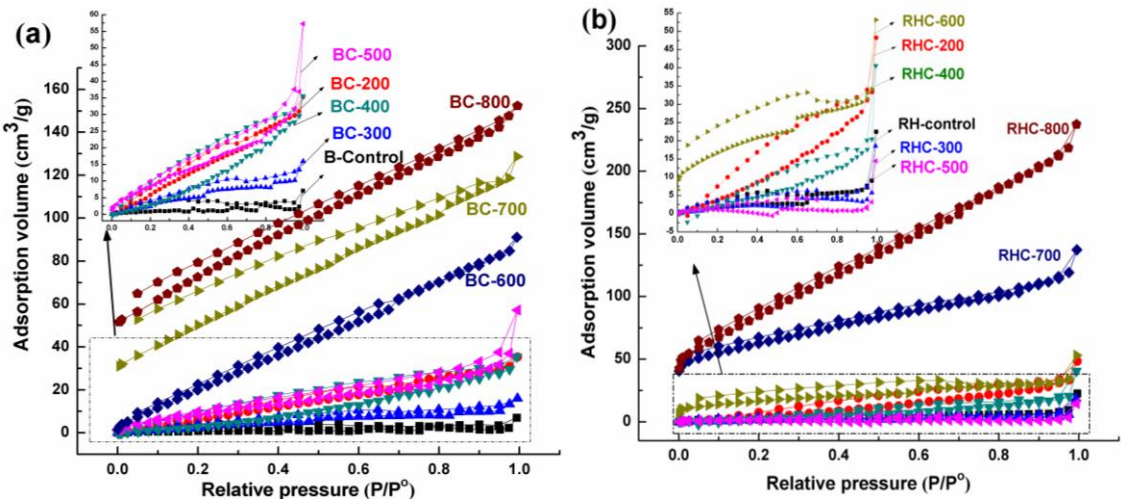

Fig. 6. Nitrogen (N_2) adsorption and desorption isotherms of BC and RHC from different pyrolysis temperatures

CONCLUSIONS

1. The physicochemical characteristics of the bio-char pyrolyzed from moso bamboo and rice husk under different pyrolysis temperatures were investigated and compared. As the temperature was increased, the bio-char yield for both BC and RHC decreased, while the carbon element content and fixed carbon, the value of HHV, and pH increased for both BC and RHC.
2. At the same pyrolysis temperature, the BC had a higher content of the carbon element and fixed carbon, and a higher value of HHV than RHC, which indicated that BC was a more suitable material for high-quality fuels and carbon sequestration carriers. However, the RHC had a higher ash content, containing 86.26 wt.% of SiO_2, which is a material with potential for use in extracting high purity amorphous silica. The pH value of the bio-chars was higher than 10 for BC-800 and RHC-800.
3. The graphitization degree of BC was higher than that of RHC. The S_{BET} for BC-800 and RHC-800 reached their maximum values of 259.89 m^2/g and 331.23 m^2/g, respectively, which indicated that BC and RHC could be an excellent interim form for activated carbon production, or use as a catalyst precursor and fuel cell material.

ACKNOWLEDGMENTS

This research was supported by the Natural Science Foundation of Zhejiang Province (LQ17E060002), the Natural 948 Project (2014-4-29), Natural Science Foundation of China (L1422039), the Fund for Innovative Research Team of Forestry Engineering Discipline (101-206001000706), and the Priority Academic Program Development of Jiangsu Higher Education Institutions (PAPD). The authors also acknowledge the Advanced Analysis & Testing Center of Nanjing Forestry University for its testing service.

REFERENCES CITED

Alvarez, J., Lopez, G., Amutio, M., Bilbao, J., and Olazar, M. (2014). "Upgrading the rice husk char obtained by flash pyrolysis for the production of amorphous silica and high quality activated carbon," *Bioresource Technology* 170, 132-137. DOI: 10.1016/j.biortech.2014.07.073

Angin, D. (2013a). "Effect of pyrolysis temperature and heating rate on biochar obtained from pyrolysis of safflower seed press cake," *Bioresource Technology* 128, 593-597. DOI: 10.1016/j.biortech.2012.10.150

Angin, D., Altintig, E., and Kose, T. E. (2013b). "Influence of process parameters on the surface and chemical properties of activated carbon obtained from biochar by chemical activation," *Bioresource Technology* 148, 542-549. DOI: 10.1016/j.biortech.2013.08.164

ASTM D1762-84 (2013). "Standard test method for chemical analysis of wood charcoal," ASTM International, West Conshohocken, USA.

Chen, D., Chen, X., Sun, J., Zheng, Z., and Fu, K. (2016a). "Pyrolysis polygeneration of pine nut shell: Quality of pyrolysis products and study on the preparation of activated carbon from biochar," *Bioresource Technology* 216, 629-636. DOI: 10.1016/j.biortech.2016.05.107

Chen, D., Li, Y., Cen, K., Luo, M., Li, H., and Lu, B. (2016b). "Pyrolysis polygeneration of poplar wood: Effect of heating rate and pyrolysis temperature," *Bioresource Technology* 218, 780-788. DOI: 10.1016/j.biortech.2016.07.049

Chen, D., Liu, D., Zhang, H., Chen, Y., and Li, Q. (2015a). "Bamboo pyrolysis using TG–FTIR and a lab-scale reactor: Analysis of pyrolysis behavior, product properties, and carbon and energy yields," *Fuel* 148, 79-86. DOI: 10.1016/j.fuel.2015.01.092

Chen, D., Mei, J., Li, H., Li, Y., Lu, M., Ma, T., and Ma, Z. (2017a). "Combined pretreatment with torrefaction and washing using torrefaction liquid products to yield upgraded biomass and pyrolysis products," *Bioresource Technology* 228, 62-68. DOI: 10.1016/j.biortech.2016.12.088

Chen, D., Cen, K., Jing, X., Gao, J., Li, C., and Ma, Z. (2017b). "An approach for upgrading biomass and pyrolysis product quality using a combination of aqueous phase bio-oil washing and torrefaction pretreatment," *Bioresource Technology* 233, 150-158. DOI: 10.1016/j.biortech.2017.02.120

Chen, D., Zhou, J., and Zhang, Q. (2014a). "Effects of heating rate on slow pyrolysis behavior, kinetic parameters and products properties of moso bamboo," *Bioresource Technology* 169, 313-319. DOI: 10.1016/j.biortech.2014.07.009

Chen, D., Zhou, J., and Zhang, Q. (2014b). "Effects of torrefaction on the pyrolysis behavior and bio-oil properties of rice husk by using TG-FTIR and Py-GC/MS," *Energy & Fuels* 28(9), 5857-5863. DOI: 10.1021/ef501189p

Chen, H., Lin, G., Chen, Y., Chen, W., and Yang, H. (2016c). "Biomass pyrolytic polygeneration of tobacco waste: Product characteristics and nitrogen transformation," *Energy & Fuels* 30(3), 1579-1588. DOI: 10.1021/acs.energyfuels.5b02255

Chen, H., Liu, D., Shen, Z., Bao, B., Zhao, S., and Wu, L. (2015b). "Functional biomass carbons with hierarchical porous structure for supercapacitor electrode materials," *Electrochimica Acta* 180, 241-251. DOI: 10.1016/j.electacta.2015.08.133

Chen, T. J., Liu, R. H., and Scott, N. R. (2016d). "Characterization of energy carriers obtained from the pyrolysis of white ash, switchgrass and corn stover - Biochar, syngas and bio-oil," *Fuel Processing Technology* 142, 124-134. DOI: 10.1016/j.fuproc.2015.09.034

Chen, Y., Yang, H., Wang, X., Zhang, S., and Chen, H. (2012). "Biomass-based pyrolytic polygeneration system on cotton stalk pyrolysis: Influence of temperature," *Bioresource Technology* 107, 411-418. DOI: 10.1016/j.biortech.2011.10.074

Cimo, G., Kucerik, J., Berns, A. E., Schaumann, G. E., Alonzo, G., and Conte, P. (2014). "Effect of heating time and temperature on the chemical characteristics of biochar from poultry manure," *Journal of Agricultural and Food Chemistry* 62(8), 1912-1918. DOI: 10.1021/jf405549z

Duman, G., Okutucu, C., Ucar, S., Stahl, R., and Yanik, J. (2011). "The slow and fast pyrolysis of cherry seed," *Bioresource Technology* 102(2), 1869-1878. DOI: 10.1016/j.biortech.2010.07.051

Fu, P., Yi, W. M., Bai, X. Y., Li, Z. H., Hu, S., and Xiang, J. (2011). "Effect of temperature on gas composition and char structural features of pyrolyzed agricultural residues," *Bioresource Technology* 102(17), 8211-9. DOI: 10.1016/j.biortech.2011.05.083

GB/T 2677.6 (1994). "Fibrous raw material-determination of solvent extractives," Standardization of Administration of China, Beijing, China.

GB/T 2677.8 (1994). "Fibrous raw material-determination of acid-insoluble lignin," Standardization of Administration of China, Beijing, China.

GB/T 2677.10 (1995). "Fibrous raw material-determination of holocellulose," Standardization of Administration of China, Beijing, China.

GB/T 12469.7 (1999). "Test methods of wooden activated carbon-determination of pH," Standardization of Administration of China, Beijing, China.

Guerrero, M., Ruiz, M. P., Millera, Á., Alzueta, M. U., and Bilbao, R. (2008). "Characterization of biomass chars formed under different devolatilization conditions: Differences between rice husk and eucalyptus," *Energy & Fuels* 22(2), 1275-1284. DOI: 10.1021/ef7005589

Kan, T., Strezov, V., and Evans, T. J. (2016). "Lignocellulosic biomass pyrolysis: A review of product properties and effects of pyrolysis parameters," *Renewable & Sustainable Energy Reviews* 57, 1126-1140. DOI: 10.1016/j.rser.2015.12.185

Kantarelis, E., Liu, J., Yang, W., and Blasiak, W. (2010). "Sustainable valorization of bamboo *via* high-temperature steam pyrolysis for energy production and added value materials," *Energy & Fuels* 24(11), 6142-6150. DOI: 10.1021/ef100875g

Krzesińska, M., and Zachariasz, J. (2007). "The effect of pyrolysis temperature on the physical properties of monolithic carbons derived from solid iron bamboo," *Journal of Analytical and Applied Pyrolysis* 80(1), 209-215. DOI: 10.1016/j.jaap.2007.02.009

Lee, Y., Park, J., Ryu, C., Gang, K. S., Yang, W., Park, Y. K., Jung, J., and Hyun, S. (2013). "Comparison of biochar properties from biomass residues produced by slow pyrolysis at 500 degrees C," *Bioresource Technology* 148, 196-201. DOI: 10.1016/j.biortech.2013.08.135

Liu, W. -J., Zeng, F. -X., Jiang, H., and Zhang, X. -S. (2011). "Preparation of high adsorption capacity bio-chars from waste biomass," *Bioresource Technology* 102(17), 8247-8252. DOI: 10.1016/j.biortech.2011.06.014

Luo, L., Xu, C., Chen, Z., and Zhang, S. Z. (2015). "Properties of biomass-derived biochars: Combined effects of operating conditions and biomass types," *Bioresource Technology* 192, 83-89. DOI: 10.1016/j.biortech.2015.05.054

Ma, Z. Q., Chen, D. Y., Gu, J., Bao, B. F., and Zhang, Q. S. (2015a). "Determination of pyrolysis characteristics and kinetics of palm kernel shell using TGA-FTIR and model-free integral methods," *Energy Conversion and Management* 89, 251-259. DOI: 10.1016/j.enconman.2014.09.074

Ma, Z. Q., Ye, J. W., Zhao, C., and Zhang, Q. S. (2015b). "Gasification of rice husk in a downdraft gasifier: The effect of equivalence ratio on the gasification performance, properties, and utilization of analysis of byproducts of char and tar," *BioResources* 10(2), 2888-2902.

Ma, Z. Q., Sun, Q. F., Ye, J. W., Yao, Q. F., and Zhao, C. (2016). "Study on the thermal degradation behaviors and kinetics of alkali lignin for production of phenolic-rich bio-oil using TGA-FTIR and Py-GC/MS," *Journal of Analytical and Applied Pyrolysis* 117, 116-124. DOI: 10.1016/j.jaap.2015.12.007

Ma, Z. Q., Zhang, Y. M., Zhang, Q. S., Qu, Y. B., Zhou, J. B., and Qin, H. F. (2012). "Design and experimental investigation of a 190 kW(e) biomass fixed bed gasification and polygeneration pilot plant using a double air stage downdraft approach," *Energy* 46(1), 140-147. DOI: 10.1016/j.energy.2012.09.008

Muhammad, N., Omar, W. N., Man, Z., Bustam, M. A., Rafiq, S., and Uemura, Y. (2012). "Effect of ionic liquid treatment on pyrolysis products from bamboo," *Industrial & Engineering Chemistry Research* 51(5), 2280-2289. DOI: 10.1021/ie2014313

Nanda, S., Dalai, A. K., Berruti, F., and Kozinski, J. A. (2016). "Biochar as an exceptional bioresource for energy, agronomy, carbon sequestration, activated carbon and specialty materials," *Waste and Biomass Valorization* 7(2), 201-235. DOI: 10.1007/s12649-015-9459-z

Oyedun, A. O., Gebreegziabher, T., and Hui, C. W. (2013). "Mechanism and modelling of bamboo pyrolysis," *Fuel Processing Technology* 106, 595-604. DOI: 10.1016/j.fuproc.2012.09.031

Paethanom, A., and Yoshikawa, K. (2012). "Influence of pyrolysis temperature on rice husk char characteristics and its tar adsorption capability," *Energies* 5(12), 4941. DOI: 10.3390/en5124941

Qian, K. Z., Kumar, A., Zhang, H. L., Bellmer, D., and Huhnke, R. (2015). "Recent advances in utilization of biochar," *Renewable & Sustainable Energy Reviews* 42, 1055-1064. DOI: 10.1016/j.rser.2014.10.074

Rafiq, M. K., Bachmann, R. T., Rafiq, M. T., Shang, Z., Joseph, S., and Long, R. (2016). "Influence of pyrolysis temperature on physico-chemical properties of corn stover (*Zea mays* L.) biochar and feasibility for carbon capture and energy balance," *Plos One* 11(6), e0156894. DOI: 10.1371/journal.pone.0156894

Ren, X. Y., Zhang, Z. T., Wang, W. L., Si, H., Wang, X., and Chang, J. M. (2013). "Transformation and products distribution of moso bamboo and derived components during pyolysis," *BioResources* 8(3), 3685-3698.

Majumder, A.K., Jain, R., Banerjee, P., and Barnwal, J. P. (2008). "Development of a new proximate analysis based correlation to predict calorific value of coal," *Fuel* 87, 3077-3081. DOI: 10.1016/j.fuel.2008.04.008

Tripathi, M., Sahu, J. N., and Ganesan, P. (2016). "Effect of process parameters on production of biochar from biomass waste through pyrolysis: A review," *Renewable & Sustainable Energy Reviews* 55, 467-481. DOI: 10.1016/j.rser.2015.10.122

Uçar, S., and Karagöz, S. (2009). "The slow pyrolysis of pomegranate seeds: The effect of temperature on the product yields and bio-oil properties," *Journal of Analytical and Applied Pyrolysis* 84(2), 151-156. DOI: 10.1016/j.jaap.2009.01.005

Wada, M., Hori, R., Kim, U. J., and Sasaki, S. (2010). "X-ray diffraction study on the thermal expansion behavior of cellulose Iβ and its high-temperature phase," *Polymer Degradation & Stability* 95(8), 1330-1334. DOI: 10.1016/j.polymdegradstab.2010.01.034

Yang, E., Jun, M., Haijun, H., and Wenfu, C. (2015). "Chemical composition and potential bioactivity of volatile from fast pyrolysis of rice husk," *Journal of Analytical and Applied Pyrolysis* 112, 394-400. DOI: 10.1016/j.jaap.2015.02.021

Yang, H. P., Huan, B. J., Chen, Y. Q., Gao, Y., Li, J., and Chen, H. P. (2016). "Biomass-based pyrolytic polygeneration system for bamboo industry waste: Evolution of the char structure and the pyrolysis mechanism," *Energy & Fuels* 30(8), 6430-6439. DOI: 10.1021/acs.energyfuels.6b00732

Zhang, J., Liu, J., and Liu, R. L. (2015). "Effects of pyrolysis temperature and heating time on biochar obtained from the pyrolysis of straw and lignosulfonate," *Bioresource Technology* 176, 288-291. DOI: 10.1016/j.biortech.2014.11.011

Zhang, S., Dong, Q., Zhang, L., and Xiong, Y. (2016). "Effects of water washing and torrefaction on the pyrolysis behavior and kinetics of rice husk through TGA and Py-GC/MS," *Bioresource Technology* 199, 352-361. DOI: 10.1016/j.biortech.2015.08.110

Zhao, Y. J., Feng, D. D., Zhang, Y., Huang, Y. D., and Sun, S. Z. (2016). "Effect of pyrolysis temperature on char structure and chemical speciation of alkali and alkaline earth metallic species in biochar," *Fuel Processing Technology* 141, 54-60. DOI: 10.1016/j.fuproc.2015.06.029

Article submitted: January 30, 2017; Peer review completed: April 13, 2017; Revised version received and accepted: May 1, 2017; Published: May 9, 2017.
DOI: 10.15376/biores.12.3.4652-4669